Frontiers of Information Technology & Electronic Engineering
www.zju.edu.cn/jzus; engineering.cae.cn; www.springerlink.com
ISSN 2095-9184 (print); ISSN 2095-9230 (online)
E-mail: jzus@zju.edu.cn

A method of shadow puppet figure modeling and animation*

Xiao-fang HUANG[1], Shou-qian SUN[1], Ke-jun ZHANG[‡1], Tian-ning XU[1], Jian-feng WU[2], Bin ZHU[3]

([1]*College of Computer Science and Technology, Zhejiang University, Hangzhou 310027, China*)

([2]*School of Art, Zhejiang University of Technology, Hangzhou 310023, China*)

([3]*College of Information Science and Technology, Zhejiang Shuren University, Hangzhou 310015, China*)

E-mail: xfhuangava@gmail.com; ssq@zju.edu.cn; channy@zju.edu.cn;
alicexutt@163.com; jianfw@126.com; zhubinxx@sohu.com

Received Oct. 15, 2014; Revision accepted Feb. 3, 2015; Crosschecked Apr. 13, 2015

Abstract: To promote the development of the intangible cultural heritage of the world, shadow play, many studies have focused on shadow puppet modeling and interaction. Most of the shadow puppet figures are still imaginary, spread by ancients, or carved and painted by shadow puppet artists, without consideration of real dimensions or the appearance of human bodies. This study proposes an algorithm to transform 3D human models to 2D puppet figures for shadow puppets, including automatic location of feature points, automatic segmentation of 3D models, automatic extraction of 2D contours, automatic clothes matching, and animation. Experiment proves that more realistic and attractive figures and animations of the shadow puppet can be generated in real time with this algorithm.

Key words: Shadow play, Shadow puppet figure, 3D human body, Data processing, 2D modeling
doi:10.1631/FITEE.1400351 **Document code:** A **CLC number:** TP391.4

1 Introduction

Shadow play is an intangible cultural heritage in the world. There are many kinds of shadow plays in Southeast Asia, Europe, the United States, some Arab countries, and other countries and regions, all with their own national characteristic features (van Ness and Prawirohardjo, 1981; Salij, 1982; Liu, 1988; Matusky, 1994; Currell, 2008; Jernigan *et al.*, 2013; Morse, 2013; Skipitares, 2013; Wang, 2013; Chen, 2014). Recently, the intangible cultural heritage of shadow play has slowly disappeared, because people lose interest in it with the increasing popularity of new media. There is a need to promote this heritage.

To attract more attention, some researchers have used multimedia and interactive tools. In general, there are two types of efforts in digitizing traditional shadow play: modeling and interactive motion controlling. The efforts in modeling include using sophisticated computer graphics techniques in OpenGL (Zhu *et al.*, 2003), modeling from a physical puppet's digital images with a high resolution (Lam *et al.*, 2008), modeling by Maya MEL animation programming language (Ghani, 2011b), and modeling by a system with a Kinect depth sensor (Held *et al.*, 2012). The efforts in interactive controlling include motion planning (Li and Hsu, 2007), visualization elements of shadow play technique movement (Ghani, 2011a), an interactive digital shadow simulation system (Li *et al.*, 2011), interactive shadow puppets play using texture mapping and blending

‡ Corresponding author

* Project partly supported by the National Natural Science Foundation of China (Nos. 61103100, 61303137, and 51205059), the Natural Science Foundation of Zhejiang Province, China (Nos. Y13F020143 and LY13F030002), and the Fundamental Research Funds for the Central Universities, China (No. 2014QNA5009)

ORCID: Xiao-fang HUANG, http://orcid.org/0000-0002-1210-7580

techniques (Talib *et al.*, 2012), and an interactive interface using the Kinect sensor (Zhang *et al.*, 2012).

Most of the shadow puppet figure models at present are still fictional and imaginary, spread by ancients, or carved and painted by shadow puppet artists, made without according to the real dimensions or appearance of human bodies. With the development of 3D scanning and personalized demands, this study proposes a method of shadow puppet figure modeling based on scanned data of real 3D human bodies to carry forward shadow play, especially in modern shadow puppet theaters or for personalized customizations, and finally realizes automatic animations.

An important innovation of our method is to extract accurate 2D contours and dimensions of human bodies from 3D models. The accurate 2D contours of shadow puppet figures can be more accurately obtained by each part of a 3D human body's projection than 2D images. However, due to the difference of body scanning postures and overlapping projections of a whole body, it is necessary to automatically identify each part of the human body and project it. The segmentation is based on feature points of the scanned model, and thus the automatic location of feature points is needed before segmentation.

After obtaining the 2D contours of shadow puppet figures, data processing, coloring, dressing, and depicting are indispensable. The framework of our approach is illustrated in Fig. 1. First, we obtain a 3D model of a human body. Then we locate the feature points of the 3D model and segment it automatically. The next steps are automatic 2D contour extraction and data processing, and automatic dressing and matching from the clothing database which we have designed. Finally, the stories and the scenes are selected from the database to generate the animation automatically.

2 Related works

From Fig. 1, we can see the preparation stage for obtaining 2D contours of shadow puppet figures including acquisition of the 3D model of the human body, location of 3D feature points, and automatic segmentation.

2.1 Location of feature points

The existing methods for 3D human body location of feature points are summarized into three categories. The first kind is using special patterns to mark human body landmarks which could be easily detected on images of the whole body surface (Geisen *et al.*, 1995; Lewark and Nurre, 1998). This kind of method is reliable, but spends time in sticking patterns and requires high-resolution scanners for reliable detection of markers. Some applications require wearing special clothes for detection. The second kind is semi-automatic prediction of landmarks on human models (Wuhrer *et al.*, 2010). The second kind is better than the first one, but the deficiency is still there. The main method used is the third one, i.e., automatic location of feature points, including template matching positioning (Allen *et al.*, 2003), geodesic distance (Katz and Tal, 2003; Katz *et al.*, 2005; Golovinskiy and Funkhouser, 2008; Shapira *et al.*, 2008), Reeb (Mortara *et al.*, 2006; Werghi *et al.*, 2006), multi-scale touch paste morphology (Gutiérrez *et al.*, 2007), and a prior knowledge (Simari *et al.*, 2009; Kalogerakis *et al.*, 2010). Compared with the former two, these automatic methods save a lot of time and have good

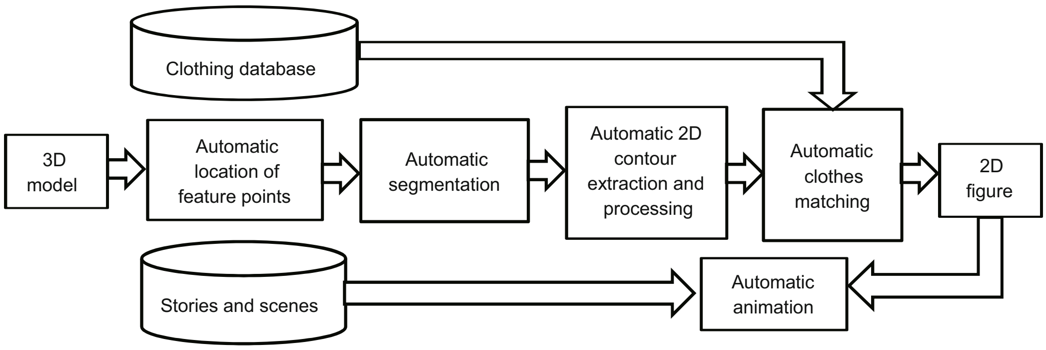

Fig. 1 The framework of our approach

generality, but need a large amount of calculations. This paper proposes a method of automatic location of feature points by partial cutting according to the range of the dimensional proportion of the standard human body in anthropometry. This saves time and reduces the amount of calculations.

2.2 Automatic segmentation

Automatic human body segmentation methods are divided mainly into two categories. One is for standard posture, such as Nurre (1997), Dekker *et al.* (1998; 1999), Nurre *et al.* (2000), and Wang *et al.* (2003). In Nurre (1997), Dekker *et al.* (1998; 1999), and Nurre *et al.* (2000), the body structure was approximated by a six-stick template; in Wang *et al.* (2003), a fuzzy logic framework was proposed. The other category is for any posture, where gesture recognition is required first. The 3D human segmentation in this study is for extracting the 2D contour. To reduce the work and improve the accuracy, the human model in our experiment is in a regular standard posture, and is segmented by the located feature points.

2.3 Shadow puppet modeling

There are four main kinds of methods for shadow puppet modeling. The first is fictional or virtual 2D modeling (Lam *et al.*, 2008). Using sophisticated computer graphics techniques available in OpenGL, it can generate interactive plays in a real-time environment and realistic animations. Although the model is created from a real image of 2D puppets, the 2D puppet is fictional, carved and painted by shadow puppet artists, and not based on physical objects. The second is real 2D modeling (Zhu *et al.*, 2003). A physical puppet's digital images with a high resolution are photographed and then these images are processed digitally for shadow play modeling. Its advantage is that 2D digital processing is relatively simple for modeling, and the model is based on physical objects. However, the disadvantage is that the model of the shadow play is restricted by 2D photographed images. Errors in the model's contour exist due to the overlapping of the 3D puppet in the 2D images. The third is virtual 3D modeling (Ghani, 2011b). Maya MEL animation programming language is used for character rigging, and it is still not based on physical objects. The fourth is real 3D modeling (Held *et al.*, 2012). A system with a Kinect depth sensor is presented for producing 3D animations using physical objects as the input. In fact, it is a track and output 3D model system.

Shadow play is usually a 2D shape. The main innovation of this study lies in shadow puppet figure modeling—a real dynamic 2D modeling based on real static 3D human scanned data. It is different from others on 2D processing and display of 3D human models (Kavan *et al.*, 2008). Kavan *et al.* (2008) was to generate and show 2D polygonal characters for rendering efficiency and visual fidelity of 3D crowds.

3 Our method

The steps include the acquisition and processing of 3D human models, automatic extraction of 2D contours and data processing, and automatic dressing and matching from the clothing database which has been designed. This method has a generality, such that it can be easily transplanted for any different human models, and clothes and actions of the generated puppet figure can be changed freely in any different scene.

3.1 Acquisition and processing of 3D human models

Three-dimensional scanned data acquisition and pretreatment are required for extracting 2D contours of the 3D human model and calculating its real dimensions. Three-dimensional data processing includes mainly automatic location of feature points and automatic segmentation.

The entire data of a human body can be obtained by a 3D scanner. The data used in this experiment was obtained by using a whole body scanner 3D Mega Capturor II LF (InSpeck Inc., Canada) (Fig. 2).

The 3D scanner connects to a computer with data lines. The data of the human model obtained can be stored in a specified model database of the computer, and can be exported to different file formats, including obj, fbx, dxf, stl, vrml, lwo, maya, hrc, and 3ds. (McHenry and Bajcsy, 2008). All these files store surface information of a human body, including points, lines, and triangular meshes. Any data of the 3D scanned models can be imported from the model database.

Because a female's body has more complexities than a male's, a female model was chosen as the experimental figure in this study (Fig. 3).

Fig. 2 The scanner 3D Mega Capturor II LF (InSpeck Inc., Canada)

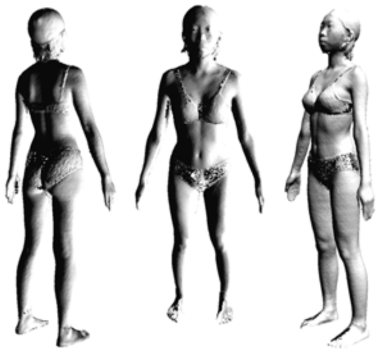

Fig. 3 The initial scanned female model

The scanned data is unordered—the orientations and the posture of the human model may be different. After obtaining the data, the next step is orientation judgment of the human body. This study considers the right side of a human body as the positive direction.

After acquiring and pretreating the scanned data, the next important step is automatic location of feature points. By analyzing the characteristics of real human bodies, this study locates feature points of the scanned model by partial cutting according to the range of the dimensional proportion of the standard human body in anthropometry. If the size of the scanned human model is not a standard one, such as having a beer belly, we will calculate the location of the feature point on a standard human body scale.

The ranges of the cutting refer to the dimensional proportion of the standard human body in anthropometry (Tilley, 1993). Different bodies have different dimensions. Each dimensional proportion is slightly different. To reduce errors, the cutting scope of the human body in this study is expanded appropriately.

Take the knee joint as an example. In anthropometry the proportion h_{99} of the perpendicular distance between the knee and the horizontal plane of the female model to the height of the whole body is 0.282 (h_{99}=(84+417)/1774=0.282). In the same way, the proportion h_{50} is 0.282 (h_{50}=(74+384)/1626=0.282). The proportion h_1 is 0.272 (h_1=(64+338)/1476=0.272).

Therefore, in anthropometry, by taking the horizontal plane as the starting plane, the range of the knee in proportion to the height of the human body is from 0.272 to 0.282. We can refer to this ratio range in positioning the knee of the 3D scanned model. Because there are individual differences between human models, to reduce the error, we can expand the scope of the positioning appropriately. In this study the scope is from 0.25 to 0.30 (Fig. 4). Within the scope, the scanned model is cut by a set of planes parallel to the horizontal plane. The distances between the adjacent planes are equal.

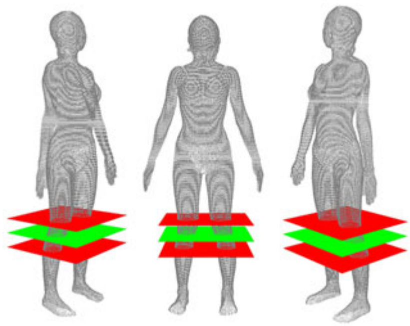

Fig. 4 The partial cutting planes in the scope

There are two methods for locating feature points in this study. One is to calculate and compare the number and the curvature of closed cycles in a cross section, such as the crotch, left oxter, and right oxter. The other is to calculate and compare the length and the curvature of the adjacent cutting circles between the body's surfaces and the cutting planes, such as the neck, shoulder, abdomen, knee, elbow, ankle, wrist, mouth, nose, and eyes. Take the crotch and the knee respectively to illustrate these two methods. The points on the cutting plane are denoted as $\{\boldsymbol{P}_i(x_i, y_i)|i = 0, 1, \ldots, n-1\}$, and then the length of circle l_c is

$$\begin{cases} l_0 = [(x_{n-1} - x_0)^2 + (y_{n-1} - y_0)^2 \\ \qquad +(z_{n-1} - z_0)^2]^{1/2}, \\ l_{i+1} = [(x_{i+1} - x_i)^2 + (y_{i+1} - y_i)^2 \\ \qquad +(z_{i+1} - z_i)^2]^{1/2}, \\ l_c = l_0 + \sum_{i=0}^{n-2} l_{i+1}. \end{cases} \tag{1}$$

By the first method, the characteristic of the knee is that its joint is swelled, and the length of the cutting circle is longer than that of the adjacent upper and lower cutting circles. Accordingly, the plane in which the knee is in is to be located by calculating the length and the curvature of the cutting circle in the cutting scope. The cross sections in which the knees are in are shown in Fig. 5.

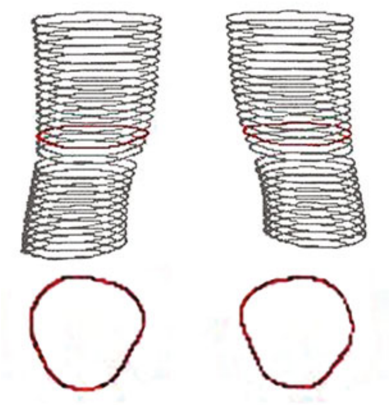

Fig. 5 The cutting circles in the scope in which the joints of the knees are

Another method for feature point positioning is calculating and comparing the number of closed circles, for example, the crotch. In the cutting scope of the crotch, the cross sections near the crotch are different. The cross section above the crotch is shown in Fig. 6a. There is one closed section. The cross section below the crotch is shown in Fig. 6b, and there are two closed circles—two legs' cross sections.

On the basis of the located feature points, the scanned model of the human body can be automatically sectioned. The details are introduced as follows.

Take the right arm as an example. There are three feature points known: one is the point of the right shoulder denoted as $\boldsymbol{P}_{\rm rs}(x_{\rm rs}, y_{\rm rs}, z_{\rm rs})$, and the other two are the point of back right oxter denoted as $\boldsymbol{P}_{\rm rb}(x_{\rm rb}, y_{\rm rb}, z_{\rm rb})$ and the point of the front right oxter denoted as $\boldsymbol{P}_{\rm rf}(x_{\rm rf}, y_{\rm rf}, z_{\rm rf})$, as shown in Fig. 7. The equation of the segmenting plane is

$$\begin{vmatrix} x - x_{\rm rs} & y - y_{\rm rs} & z - z_{\rm rs} \\ x_{\rm rf} - x_{\rm rs} & y_{\rm rf} - y_{\rm rs} & z_{\rm rf} - z_{\rm rs} \\ x_{\rm rb} - x_{\rm rs} & y_{\rm rb} - y_{\rm rs} & z_{\rm rb} - z_{\rm rs} \end{vmatrix} = 0. \tag{2}$$

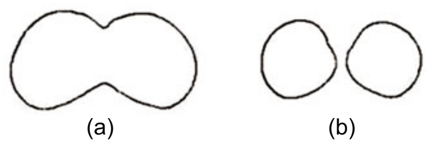

Fig. 6 The cross sections above (a) and below (b) the crotch

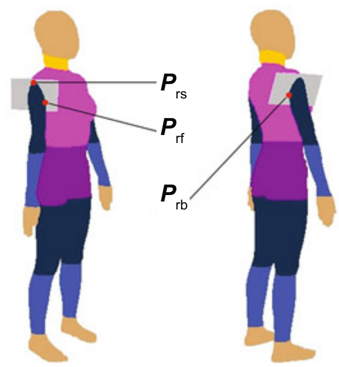

Fig. 7 The cutting plane of the right arm

The right arm is automatically separated from the whole model by the segmenting plane. In the same way, the other parts of the model can be separated. The 3D human model in this study is divided into 16 different parts for movement agility: the head, neck, chest, abdomen, upper left arm, upper right arm, lower left arm, lower right arm, left hand, right hand, upper left leg, upper right leg, lower left leg, lower right leg, left foot, and right foot (Fig. 8).

We select 120 students in our university as experimental objects. Their heights are from 156 to 182 cm. Their positions of feature points are measured manually before scanning for comparison with automatic locations to test the error and effectiveness of the algorithm. The experimental results show that the error is between −0.9 and +0.7 cm, and the average time for automatic measurement is less than 0.1% of the manual measurement. The average calculation in the process of automatic measurement is lower than 1% compared with other automatic segmentation algorithms.

3.2 Automatic extraction of 2D contours

The main characteristic of shadow play is 2D. All the parts of the body are linked by joints. After the location of feature points and automatic segmentation, the contours and the dimensions of the shadow puppet figure can be calculated and measured automatically. The shadow puppet figure is always sideways at five tenths—the proportion of the projected 2D facial area to the entire 3D facial area is five to ten, with a small number of six tenths, seven tenths, eight tenths, or even a whole front face. This ratio is determined by the projection plane. If the operators want to display a different percentage, they will select the corresponding projection plane, and the other steps and algorithms are the same. Here we choose sideways at five tenths of the face commonly used in shadow puppet making for the experiment. All the projection planes of the human model are shown in Fig. 9.

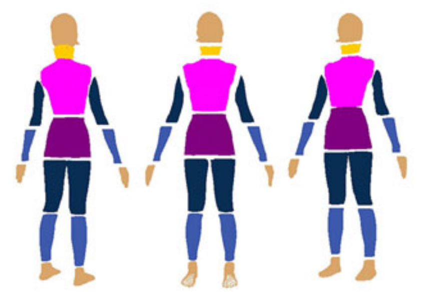

Fig. 8 The results of automatic segmentation

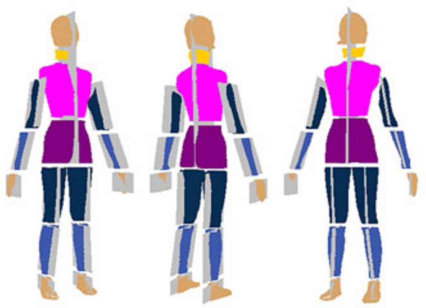

Fig. 9 The projection planes

Take the upper right arm as an example. The joints of upper right arm $\boldsymbol{P}_{\rm ura}(x_{\rm ura}, y_{\rm ura}, z_{\rm ura})$, the front right elbow $\boldsymbol{P}_{\rm fre}(x_{\rm fre}, y_{\rm fre}, z_{\rm fre})$, and the back right elbow $\boldsymbol{P}_{\rm bre}(x_{\rm bre}, y_{\rm bre}, z_{\rm bre})$ have been known. The equation of the projection plane is

$$\begin{vmatrix} x - x_{\rm ura} & y - y_{\rm ura} & z - z_{\rm ura} \\ x_{\rm fre} - x_{\rm ura} & y_{\rm fre} - y_{\rm ura} & z_{\rm fre} - z_{\rm ura} \\ x_{\rm bre} - x_{\rm ura} & y_{\rm bre} - y_{\rm ura} & z_{\rm bre} - z_{\rm ura} \end{vmatrix} = 0. \quad (3)$$

As shown in Fig. 10, the coordinates of the 3D human model are represented as $X_{\rm h}Y_{\rm h}Z_{\rm h}$. The plane $P_{\rm bre}P_{\rm ure}P_{\rm ura}$ is the projection plane of the upper right arm. $X_{\rm f}O_{\rm f}Y_{\rm f}$ are the coordinates of the 2D shadow puppet figure.

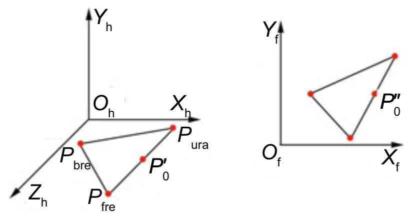

Fig. 10 The coordinate systems of the projection plane

Take one point $\boldsymbol{P}_0(x_0, y_0, z_0)$ on the upper right arm as an example. First, put $\boldsymbol{P}_0$ from the human coordinate system $X_{\rm h}Y_{\rm h}Z_{\rm h}$ to the projection plane $P_{\rm bre}P_{\rm ura}P_{\rm fre}$. The new coordinates of $\boldsymbol{P}_0$ are denoted as $\boldsymbol{P}_0'(x_0', y_0', z_0')$. Then the values of $\boldsymbol{P}_0'$ in the plane $P_{\rm bre}P_{\rm ura}P_{\rm fre}$ are shown in Eqs. (4) and (5):

$$\begin{bmatrix} x_0' \\ y_0' \\ z_0' \end{bmatrix}^{\rm T} = -\frac{a \cdot x_0 + b \cdot y_0 + c \cdot z_0 + d}{a^2 + b^2 + c^2} \begin{bmatrix} a \\ b \\ c \end{bmatrix}^{\rm T} + \begin{bmatrix} x_0 \\ y_0 \\ z_0 \end{bmatrix}^{\rm T}, \quad (4)$$

$$\begin{cases} a = (y_{\rm fre} - y_{\rm ura}) \cdot (z_{\rm bre} - z_{\rm ura}) \\ \quad\; -(y_{\rm bre} - y_{\rm ura}) \cdot (z_{\rm fre} - z_{\rm ura}), \\ b = (z_{\rm fre} - z_{\rm ura}) \cdot (x_{\rm bre} - x_{\rm ura}) \\ \quad\; -(z_{\rm bre} - z_{\rm ura}) \cdot (x_{\rm fre} - x_{\rm ura}), \\ c = (x_{\rm fre} - x_{\rm ura}) \cdot (y_{\rm bre} - y_{\rm ura}) \\ \quad\; -(x_{\rm bre} - x_{\rm ura}) \cdot (y_{\rm fre} - y_{\rm ura}), \\ d = -a \cdot x_{\rm ura} - b \cdot y_{\rm ura} - c \cdot z_{\rm ura}. \end{cases} \quad (5)$$

Second, rotate the point $\boldsymbol{P}_0'(x_0', y_0', z_0')$ of the upper right arm in the plane $P_{\rm bre}P_{\rm ura}P_{\rm fre}$ to the plane $X_{\rm h}O_{\rm h}Y_{\rm h}$. The angle between the two planes is denoted as θ, the new coordinates are denoted as $\boldsymbol{P}_0''(x_0'', y_0'', z_0'')$, and the values are shown in Eqs. (6) and (7):

$$\begin{bmatrix} x_0'' \\ y_0'' \\ z_0'' \end{bmatrix}^{\rm T} = \begin{bmatrix} \sqrt{x_0'^2 + y_0'^2 + z_0'^2} \\ \sqrt{x_0'^2 + y_0'^2 + z_0'^2} \\ 0 \end{bmatrix}^{\rm T} \begin{bmatrix} \cos\theta & 0 & 0 \\ 0 & \sin\theta & 0 \\ 0 & 0 & 0 \end{bmatrix}, \quad (6)$$

$$\cos\theta = \frac{c}{\sqrt{a^2+b^2+c^2}},\ \sin\theta = \frac{\sqrt{a^2+b^2}}{\sqrt{a^2+b^2+c^2}}. \quad (7)$$

Third, map the point $\boldsymbol{P}_0''(x_0'', y_0'', z_0'')$ of the upper right arm in the plane $P_{\rm bre}P_{\rm ura}P_{\rm fre}$ to the new 2D coordinate system $X_{\rm f}O_{\rm f}Y_{\rm f}$, and the new 2D coordinates are $\boldsymbol{P}_{\rm f}(x_{\rm f}, y_{\rm f})$. Then the coordinates of $\boldsymbol{P}_{\rm f}$ in $X_{\rm f}O_{\rm f}Y_{\rm f}$ are (x_0'', y_0''). All the parts of the human scanned model in the 3D coordinates $X_{\rm h}Y_{\rm h}Z_{\rm h}$ are projected into the 2D coordinates $X_{\rm f}O_{\rm f}Y_{\rm f}$ in the same way.

The contours include not only each section's outline of borders, but also the facial organs' contour. The head projection needs to consider the facial features in addition to its outer contour. The detailed processing is as follows. Take the apex nasi, i.e., the highest point of the nose, as the equally dividing point. The lateral projection plane of the head contains the apex nasi, and its direction parallels the positive direction of the human body. Then put the eyes, nose, mouth, and ears on the projection plane. The 2D contours are shown in Fig. 11.

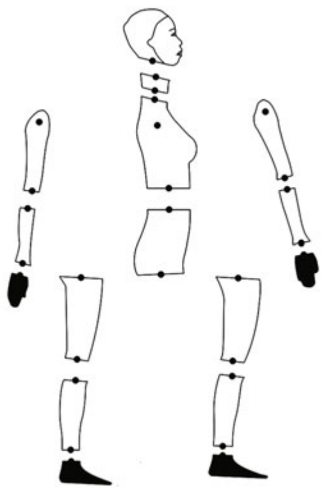

Fig. 11 The contours of all segments

After obtaining the initial 2D contours, data processing is needed for the shadow puppet figure, including resampling, standard posture recovery, joint link processing, 2D location of feature points, and dimension measurement. The details are introduced as follows.

Overlapping points exist after the projection from 3D space to 2D plane. So, the first step of 2D data processing is resampling—getting rid of the redundant data and simplifying the data volume. Take the upper left leg as an example, denoted as $\{\boldsymbol{P}_{{\rm l}_i}(x_i, y_i)|i = 0, 1, \ldots, N_{\rm l} - 1\}$. First, order the 2D projection data vertically, $\{\boldsymbol{P}_{{\rm l}_i}(x_i, y_i)|i = 0, 1, \ldots, N_{\rm l} - 1\}$, $y_i \le y_{i+1}$. Then cut the projection area with a set of parallel lines. The function of the line is

$$y_j = \frac{(y_{\max} - y_{\min}) \cdot j}{N_{\rm l}},\ j = 0, 1, \ldots, N_{\rm l} - 1, \quad (8)$$

where the minimum and maximum values of the Y axis are denoted as $y_{\min}$ and $y_{\max}$, respectively. If $|y_i - y_j| \le \epsilon$ (ϵ is set to 0.001 in this study, which is the minimum error), then $y_i = y_j$. Keep each starting point $\boldsymbol{P}_{\min_j}(x_{\min}, y_j)$ and the end point $\boldsymbol{P}_{\max_j}(x_{\max}, y_j)$ on the cutting lines, as shown in Fig. 12a. Save all the new points in clockwise order.

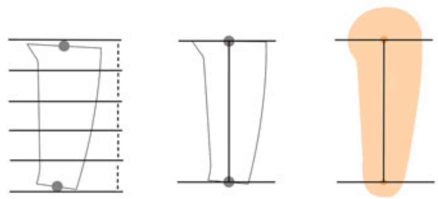

Fig. 12 The 2D data processing of the upper left leg: (a) resampling; (b) standard posture recovery; (c) joint linking

Because of the different postures of the 3D scanned human models, the postures of the contours calculated are different, and standard posture recovery is needed. The steps are as follows: calculate the center of the upper and lower boundaries of each section (standard posture recovery); link two center points of each section as the centerline; rotate each section around the centerline as the axis of rotation until the centerline is parallel to the horizontal plane (Fig. 12b).

From Fig. 11, we can see that neither end of the projection of each section is smooth. Then the next step is joint link processing—an arc surface patch is added to each end edge of a section's projection; the center is its joint in the middle of the end edge (Fig. 12c). After the above 2D data processing, the function of the curve of the contour can be calculated as

$$y_i = f_i(x) = \frac{y_{i+1} - y_i}{x_{i+1} - x_i} \cdot x + \frac{x_{i+1} \cdot y_i - x_i \cdot y_{i+1}}{x_{i+1} - x_i},$$
$$x_i \le x \le x_{i+1},\ i = 0, 1, \ldots, N_{\rm l} - 2. \quad (9)$$

The final steps of data processing are all the 2D key point locating positions and dimension measurement for matching with clothes. All the 2D key points need to be located. Some of the feature points have been labelled, and some are newly added. The method of feature point positioning for the 2D contour is as follows: calculate the curvature of the contour, and then compare it with other contours' curvatures. Take the abdomen $\{\boldsymbol{P}_{\mathrm{a}_i}(x_i, y_i)|i = 0, 1, \ldots, N_{\mathrm{a}} - 1\}$ as an example. The curvature σ_i is

$$\sigma_i = \frac{y_{i+1} - y_i}{x_{i+1} - x_i},\ i = 0, 1, \ldots, N_{\mathrm{a}} - 2. \tag{10}$$

The 2D initial naked figure of the shadow puppet is shown in Fig. 13. The results show that our approach is more accurate compared with the method of obtaining 2D contours of the human body from 2D images. It overcomes the overlaps of each section from 2D images, and calculates the precise dimensions of the contours of 3D human models with a small and negligible error.

Fig. 13 All the contours after reprocessing

3.3 Automatic clothes matching of shadow puppet figures

After contour extraction of the shadow puppet figure, automatic processing, and dimension measurement, we need to have each part colored and design clothes. The clothes of the database have been designed according to the segments of the shadow puppet figure and the feature points set in this study. The clothes matching of the shadow puppet figure can be achieved by two methods from the database of the clothes designed in this study.

One is the complete pattern matching—all the patterns of the clothes selected from the database will map to the naked shadow puppet figure; the other is partial pattern matching—keeping the main pattern of the clothes selected from the database unchanged. With the first matching method, the pattern will basically be deformed because of the different body sizes of human models, but the entire pattern will be kept. With the second method, some patterns on the clothes will be discarded, but the main pattern will be undeformed. Both of them are matching according to the contours and dimensions of the 2D shadow puppet figure. The two methods will be respectively introduced with a detailed explanation in the following.

The first method includes the proportion calculation for each relevant size between the naked contours and the matched clothes, scaling each part of the clothes vertically and horizontally, and mapping key points using the function of the contours.

To show the shape of the body, we design a cheongsam for the shadow puppet figure according to its contours and dimensions. The points' set of the chest is $\{\boldsymbol{P}_i(x_{\mathrm{p}i}, y_{\mathrm{p}i})|i = 0, 1, \ldots, N - 1\}$. The ancient costume in the database also has dimensions and key points. The points' set of the chest in the cheongsam is $\{\boldsymbol{Q}_i(x_{\mathrm{q}i}, y_{\mathrm{q}i})|i = 0, 1, \ldots, N - 1\}$. The new coordinates of the abdomen's points matching with clothes are denoted as $\{\boldsymbol{P}'_i(x'_{\mathrm{p}i}, y'_{\mathrm{p}i})|i = 0, 1, \ldots, N - 1\}$. Some key dimensions of the abdomen for the 2D puppet figure are denoted as $W_{\mathrm{p}i}$, $W_{\mathrm{p}j}$, $W_{\mathrm{p}k}$, $H_{\mathrm{p}i}$, $H_{\mathrm{p}j}$, $H_{\mathrm{p}k}$ (Fig. 14a). The key dimensions of the cheongsam on the abdomen in the database are denoted as $W_{\mathrm{q}i}$, $W_{\mathrm{q}j}$, $W_{\mathrm{q}k}$, $H_{\mathrm{q}i}$, $H_{\mathrm{q}j}$, $H_{\mathrm{q}k}$ (Fig. 14b).

In the method, first, the area of the contour according to the key points is divided into three regions: the upper arc section PI, the middle section PJ, and the lower section PK; in the same way, the clothes to be matched are divided into QI, QJ, and QK. Next, a corresponding relation is obtained by calculating the size of the measured data on each region: $W_{\mathrm{p}i}=S_{\mathrm{w}i}\cdot W_{\mathrm{q}i}$, $H_{\mathrm{p}i}=S_{\mathrm{h}i}\cdot H_{\mathrm{q}i}$. Then scale each region according to the proportion coefficient. The clothes are matched according to the proportion coefficient of each horizontal line; the starting point and the end point on each horizontal line are divided equally from top to bottom, $W'_{\mathrm{q}x} = W_{\mathrm{q}x}\,\cdot$

S_{wj} (Fig. 14c). Finally, the pattern of clothes region is mapped to the shadow play figures on the corresponding area (Fig. 14d). The 2D transformation matrix is

$$\begin{bmatrix} x'_{pi} \\ y'_{pi} \\ 1 \end{bmatrix} = \begin{bmatrix} x'_{qi} \\ y'_{qi} \\ 1 \end{bmatrix} \begin{bmatrix} 1 & 0 & 0 \\ 0 & S_{hi} & 0 \\ 0 & 0 & 1 \end{bmatrix} = \begin{bmatrix} x_{qi} \\ y_{qi} \\ 1 \end{bmatrix} \begin{bmatrix} S_{wi} & 0 & 0 \\ 0 & S_{hi} & 0 \\ 0 & 0 & 1 \end{bmatrix}. \tag{11}$$

The corresponding key points of the 2D clothes outlined map with the key points of the 2D shadow puppet figure's contours, respectively. The rest of the points also map with each other according to the corresponding relationship between key points. The same processing is done for the abdomen, neck, and other segments. By repeating such processing, all the parts can be matched.

The second method includes the proportion calculation of the whole relevant size between the naked contours and matched clothes, scaling the whole clothes, and mapping key points according to the function of the contours.

Fig. 15 shows an example of matching the cheongsam on the abdomen. First the area of the contour is divided into three regions according to the key points: PI, PJ, and PK (Fig. 15a). In the same way the clothes are divided into QI, QJ, and QK (Fig. 15b). Then the minimum bounding box of each section is calculated for the contour and cheongsam according to their key points and outline's function. The areas of the box calculated, S_{pi}, S_{pj}, S_{pk}, are the areas of the contour's boxes $A_{pi}B_{pi}C_{pi}D_{pi}$, $A_{pj}B_{pj}C_{pj}D_{pj}$, $A_{pk}B_{pk}C_{pk}D_{pk}$ respectively; S_{qi}, S_{qj}, S_{qk} are the areas of the cheongsam's boxes $A_{qi}B_{qi}C_{qi}D_{qi}$, $A_{qj}B_{qj}C_{qj}D_{qj}$, $A_{qk}B_{qk}C_{qk}D_{qk}$ respectively; and the proportion of the corresponding bounding box's area is obtained, denoted as S_i, S_j, S_k, $S_i=S_{pi}/S_{qi}$, $S_j=S_{pj}/S_{qj}$, $S_k=S_{pk}/S_{qk}$. Compare and select the maximum value among S_i, S_j, S_k, denoted as S_{max}. The whole pattern of each region is scaled within the proportion coefficient S_{max}, while keeping the shape of all the clothes unchanged; the horizontal and vertical proportions in the pattern have not changed, and the points of the contour are all in the region of the clothes (Fig. 15c). Finally, the part pattern of clothes is mapped to the shadow play figure on the corresponding area according to the function of the contours (Fig. 15d), and the 2D transformation matrix is shown in Eqs. (12)–(15). The proportion of the pattern in mapping to the

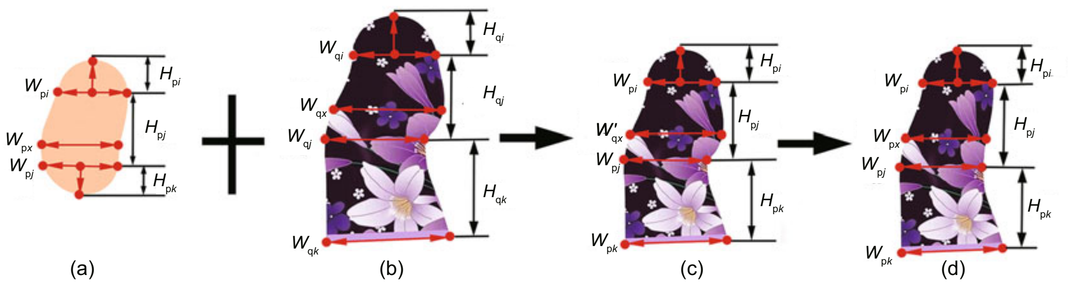

Fig. 14 The first mapping method between the contours and clothes: (a) naked abdomen of the shadow puppet figure; (b) matched clothes of the abdomen; (c) scaling the matched clothes; (d) final matched result

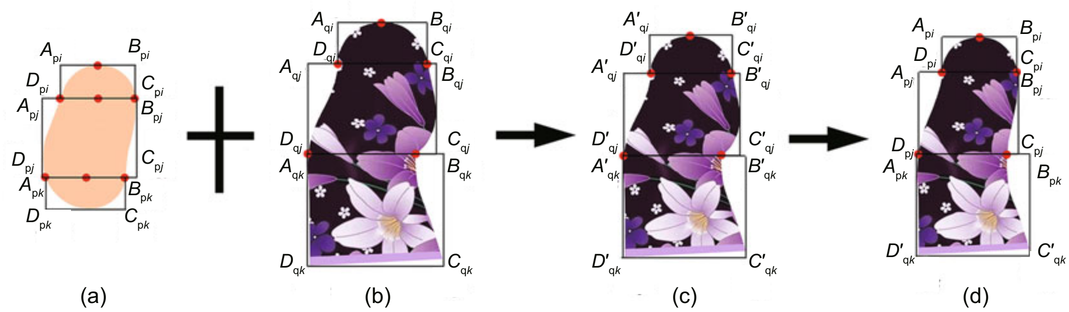

Fig. 15 The second mapping method between the contours and the clothes: (a) naked abdomen of the shadow puppet figure; (b) matched clothes of the abdomen; (c) scaling the matched clothes; (d) final matched result

naked figure, η, is calculated using Eq. (16).

$$\begin{bmatrix} x'_{qi} \\ y'_{qi} \\ 1 \end{bmatrix} = \begin{bmatrix} x_{qi} \\ y_{qi} \\ 1 \end{bmatrix} \begin{bmatrix} \sqrt{S_{\max}} & 0 & 0 \\ 0 & \sqrt{S_{\max}} & 0 \\ 0 & 0 & 1 \end{bmatrix}, \quad (12)$$

$$\begin{bmatrix} x'_{pi} \\ y'_{pi} \\ 1 \end{bmatrix} = \begin{bmatrix} x'_{qc} \\ y'_{qc} \\ 1 \end{bmatrix} + \begin{bmatrix} x_{pc} \\ y_{pc} \\ 1 \end{bmatrix} - \begin{bmatrix} x_{pi} \\ y_{pi} \\ 1 \end{bmatrix}, \quad (13)$$

$$x_{pc} = \frac{1}{n}\sum_{i=0}^{n} x_{pi}, \; y_{pc} = \frac{1}{n}\sum_{i=0}^{n} y_{pi}, \quad (14)$$

$$x'_{qc} = \frac{1}{n}\sum_{i=0}^{n} x'_{qi}, \; y'_{qc} = \frac{1}{n}\sum_{i=0}^{n} y'_{qi}, \quad (15)$$

$$\eta = \frac{\int_{x'_{p0}}^{x'_{p(n-1)}} f'_p(x'_p)\mathrm{d}x'_p}{S_{\max} \cdot \int_{x_{q0}}^{x_{q(n-1)}} f_q(x_q)\mathrm{d}x_q} \times 100\%. \quad (16)$$

In the same way, different clothes, hats, shoes, and other ornaments designed for shadow puppet figures in scenarios according to their real dimensions obtained from scanned data can be realized (Fig. 16). Using the two key points for the reference to measure the scaling proportion and the rotation angle, the hair is scaled and rotated to match the head of the shadow puppet figure. Also, the clothes in the database can be designed and updated based on the available human data.

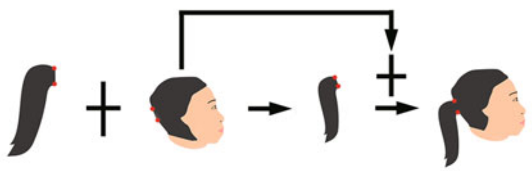

Fig. 16 Map between the head and hair accessories

All the parts of the shadow puppet figure in this study are linked by joints. The motion of the figure can be controlled by the rotating angles of joints constrained by kinesiology. Then the animation could be generated automatically after selecting stories and scenarios.

Suppose that all the points of the 3D human model are $\{\boldsymbol{P}_i(x_i, y_i, z_i)|i = 0, 1, \ldots, N_{3d}-1\}$, where N_{3d} is the number of the points, and that all the points of the 3D human model are $\{\boldsymbol{P}'_i(x'_i, y'_i)|i = 0, 1, \ldots, N_{2d} - 1\}$, where N_{2d} is the number of the points. Our method can be described as in Algorithm 1.

Algorithm 1 Processing of our method

Input: The data of the 3D human model $\{\boldsymbol{P}_i(x_i, y_i, z_i)|i = 0, 1, \ldots, N_{3d} - 1\}$

Output: The data of the shadow puppet figure $\{\boldsymbol{P}'_i(x'_i, y'_i)|i = 0, 1, \ldots, N_{2d} - 1\}$

Step 1: Preparation

1.1 Locate the feature points of the 3D human model

1.2 Segment the 3D human model into 16 parts automatically according to its key feature points

Step 2: 2D contour extraction

2.1 Position the projection plane of each segment according to its key feature points

2.2 Map each 3D segment to its projection plane, and then obtain its 2D contours

Step 3: Data processing

3.1 Resample the initial contours

3.2 Transform each contour to a standard posture

3.3 Process each joint link, and then obtain the new contours of the 2D figure, denoted as $\{\boldsymbol{P}_i(x_i, y_i)|i = 0, 1, \ldots, N_f - 1\}$

3.4 Label all the 2D key points for the next step (clothes matching)

Step 4: Clothes matching

Obtain the data of shadow puppet figure

Step 5: Select stories and scenes

Generate animation automatically

4 Experimental results

One hundred and twenty students aged from 18 to 29 years old in our university have participated in the experiment and their interest and satisfaction in the shadow puppet play were investigated with our method. The process of the experiment is as follows: the human body being scanned with simple underwear or tight clothes stands in the center with enough space between arms, legs, and the main body. The scanned data can be transferred to the database in the computer through data lines. The operator can choose the model to extract its 2D contours and choose the clothes, story, and scene in the already designed database. Then the shadow play animation will be automatically generated. Figs. 17 and 18 both show a series of the shadow puppet figure animations generated with a female model. Fig. 19 is generated with a male model. The figures, clothes, scene, and quantity of shadow play figures are freely chosen. The average number of points of the models in the experiment, time complexity, and average computation time in each processing are shown in Table 1.

Fig. 17 An animation of the female puppet figure

Fig. 18 Another animation of the female puppet figure

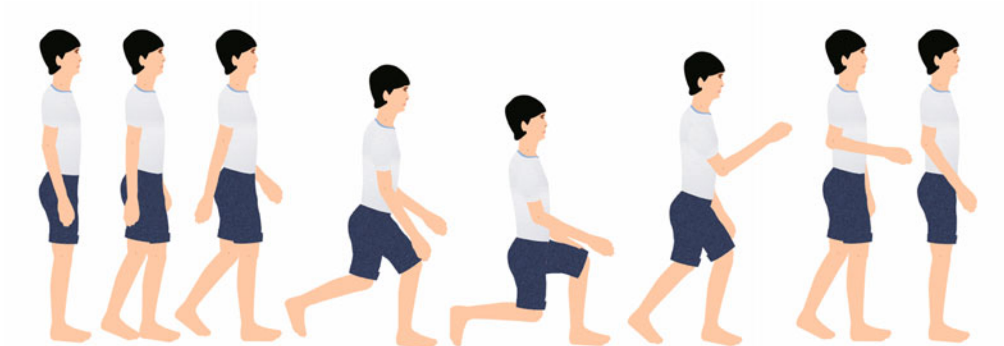

Fig. 19 The animation of the male puppet figure

The interest degree of the shadow puppet play in our questionnaire was divided into three types, i.e., not interested, a little interested, and very interested. The results of the questionnaire on degree of interest are shown in Table 2. The experimental results showed that the proportion of 'very interested' in the shadow puppet play with our method is up to 100%; compared with virtual models, more people were interested in real shadow puppets with different optional characters modeling and real-time animations. Since some of the subjects will have different cultures and backgrounds, the percentage of the interest in shadow play may have a small error, but the participants of the shadow play in modeling and animation with our method showed a strong interest in the experiment.

5 Conclusions and future work

Real modeling and real-time animations of shadow puppet figures based on real dimensions of human bodies obtained from 3D scanned data are attracting more people. With the method proposed in this paper, realistic figures of shadow puppets can be made and played not only in real shadow plays but also in digital animations. It is a natural and novel way of promoting the classic cultural treasure. This method can be applied to other shadow play animals' making and animation. Based on our experiments, the respondents involved are very interested and satisfied. In the future, more types of human models such as aged people and children, even animals, will be researched; the facial expression and makeup of the shadow puppet figure can be researched for a more fascinating image or an exaggerated design according to the need. More stories, scenes, and effects such as lighting could be added. The operation of the shadow puppet figure can also be combined with interactive technologies.

Table 1 Average number of points, time complexity, and average runtime for the different processing steps*

Processing step	Average number of points	Time complexity	Average runtime (ms)
Automatic segmentation	282 676	$O(\log n)$	8.3
Automatic 2D contour extraction	282 676	$O(\log n)$	7.5
Automatic clothes matching	87 532	$O(n)$	3.1
Automatic animation	87 532	$O(n)$	2 ms/frame

* Setting: Intel Core i5-2520M CPU 2.50 GHz with 4 GB of main memory in Visual Studio 2010

Table 2 The results of the questionnaire for the interest degree

Interest degree	Number of experimental subjects	Percentage (%)
Not interested	0	0
A little interested	2	1.67
Very interested	118	98.33

References

Allen, B., Curless, B., Popović, B., 2003. The space of human body shapes: reconstruction and parameterization from range scans. *ACM Trans. Graph.*, **22**(3):587-594. [doi:10.1145/882262.882311]

Chen, T.K., 2014. A case study of a digital archives programme: the development of digital shadow plays in Taiwan. *Int. J. Human. Arts Comput.*, **8**(suppl):38-48. [doi:10.3366/ijhac.2014.0098]

Currell, D., 2008. Shadow Puppets & Shadow Play. Crowood Press, UK.

Dekker, L., Khan, S., West, E., *et al.*, 1998. Models for understanding the 3D human body form. Proc. Int. Conf. on Computer Vision, p.65-74.

Dekker, L., Douros, I., Buston, B.F., *et al.*, 1999. Building symbolic information for 3D human body modeling from range data. Proc. 2nd Int. Conf. on 3-D Digital Imaging and Modeling, p.388-397. [doi:10.1109/IM.1999.805369]

Geisen, G.R., Mason, C.P., Houston, V.L., *et al.*, 1995. Automatic detection, identification, and registration of anatomical landmarks. Proc. Human Factors and Ergonomics Society Annual Meeting, p.750-753. [doi:10.1177/154193129503901107]

Ghani, D.A., 2011a. A study of visualization elements of shadow play technique movement and computer graphic imagery (CGI) in Wayang Kulit Kelantan. *Int. J. Comput. Graph. Animat.*, **1**(1):1-11.

Ghani, D.A., 2011b. Wayang Kulit: digital puppetry character rigging using Maya MEL language. Proc. 4th Int. Conf. on Modeling, Simulation and Applied Optimization, p.1-5. [doi:10.1109/ICMSAO.2011.5775499]

Golovinskiy, A., Funkhouser, T., 2008. Randomized cuts for 3D mesh analysis. *ACM Trans. Graph.*, **27**(5), Article 145. [doi:10.1145/1409060.1409098]

Gutiérrez, M., García-Rojas, A., Thalmann, D., *et al.*, 2007. An ontology of virtual humans. *Vis. Comput.*, **23**(3):207-218. [doi:10.1007/s00371-006-0093-4]

Held, R.T., Gupta, A., Curless, B., *et al.*, 2012. 3D puppetry: a Kinect-based interface for 3D animation. UIST, p.423-434.

Jernigan, D.K., Chansavang, A., Martin-Rall, H., *et al.*, 2013. Aesthetic affordances: computer animation and Wayang Kulit puppet theatre. *Animat. Pract. Process Product.*, **3**(1-2):195-217. [doi:10.1386/ap3.3.1-2.195_1]

Kalogerakis, E., Hertzmann, A., Singh, K., 2010. Learning 3D mesh segmentation and labeling. *ACM Trans. Graph.*, **29**(4), Article 102. [doi:10.1145/1778765.1778839]

Katz, S., Tal, A., 2003. Hierarchical mesh decomposition using fuzzy clustering and cuts. *ACM Trans. Graph.*, **22**(3):954-961. [doi:10.1145/882262.882369]

Katz, S., Leifman, G., Tal, A., 2005. Mesh segmentation using feature point and core extraction. *Vis. Comput.*, **21**(8-10):649-658. [doi:10.1007/s00371-005-0344-9]

Kavan, L., Dobbyn, S., Collins, S., *et al.*, 2008. Polypostors: 2D polygonal impostors for 3D crowds. Proc. Symp. on Interactive 3D Graphics and Games, p.149-155. [doi:10.1145/1342250.1342273]

Lam, T.K., Talib, A.Z., Osman, M.A., 2008. Real-time visual simulation and interactive animation of shadow play puppets using OpenGL. *World Acad. Sci. Eng. Technol.*, **21**:212-218.

Lewark, E.A., Nurre, J.H., 1998. Automated fudicial labeling on human body data. Proc. SPIE, p.82-89. [doi:10.1117/12.302440]

Li, Q., Hua, Q.Y., Feng, J., *et al.*, 2011. Design and implementation of interactive digital shadow simulation system. Proc. Int. Conf. on Electric and Electronics, p.187-194. [doi:10.1007/978-3-642-21762-3_24]

Li, T.Y., Hsu, S.W., 2007. An authoring tool for generating shadow play animations with motion planning techniques. *Int. J. Innov. Comput. Inform. Contr.*, **3**(6B):1601-1612.

Liu, J.L., 1988. Chinese Shadow Puppet Plays. Morning Glory Publishers, China (in Chinese).

Matusky, P., 1994. Malaysian Shadow Play and Music: Continuity of an Oral Tradition. South-East Asian Social Science Monographs. Oxford University Press, Kuala Lumpur.

McHenry, K., Bajcsy, P., 2008. An Overview of 3D Data Content, File Formats and Viewers. Technical Report, National Center for Supercomputing Applications, Urbana, USA.

Morse, L., 2013. The shadow puppet theatre of Malaysia: a study of Wayang Kulit with performance scripts and puppet designs. *Theat. J.*, **65**(1):137-138.

Mortara, M., Patané, G., Spagnuolo, M., 2006. From geometric to semantic human body models. *Comput. Graph.*, **30**(2):185-196. [doi:10.1016/j.cag.2006.01.024]

Nurre, J.H., 1997. Locating landmarks on human body scan data. Proc. Int. Conf. on Recent Advances in 3-D Digital Imaging and Modeling, p.289-295. [doi:10.1109/IM.1997.603878]

Nurre, J.H., Connor, J., Lewark, E.A., *et al.*, 2000. On segmenting the three-dimensional scan data of a human body. *IEEE Trans. Med. Imag.*, **19**(8):787-797. [doi:10.1109/42.876304]

Salij, H.J., 1982. Shadow Play and Other Stories. Heinemann Asia, Singapore.

Shapira, L., Shamir, A., Cohen-Or, D., 2008. Consistent mesh partitioning and skeletonisation using the shape diameter function. *Vis. Comput.*, **24**(4):249-259. [doi:10.1007/s00371-007-0197-5]

Simari, P., Nowrouzezahrai, D., Kalogerakis, E., *et al.*, 2009. Multi-objective shape segmentation and labeling. *Comput. Graph. Forum*, **28**(5):1415-1425. [doi:10.1111/j.1467-8659.2009.01518.x]

Skipitares, T., 2013. A new aesthetic in Indian puppetry. *PAJ*, **35**(3):61-68. [doi:10.1162/PAJJ_a_00162]

Talib, A.Z., Osman, M.A., Tan, K.L., *et al.*, 2012. Design and development of an interactive virtual shadow puppet play. Proc. 2nd Int. Conf. on Arts and Technology, p.118-126. [doi:10.1007/978-3-642-33329-3_14]

Tilley, A.R., 1993. The Measure of Man and Woman: Human Factors in Design. Whitney Library of Design, New York.

van Ness, E., Prawirohardjo, S., 1981. Javanese Wayang Kulit: an Introduction. Oxford University Press, USA.

Wang, C.C.L., Chang, T.K.K., Yuen, M.M.F., 2003. From laser-scanned data to feature human model: a system based on fuzzy logic concept. *Comput.-Aid. Des.*, **35**(3):241-253. [doi:10.1016/S0010-4485(01)00209-3]

Wang, I.C., 2013. Globalization and theater spectacles in Asia. *CLCWeb: Compar. Liter. Cult.*, **15**(2), Article 22. [doi:10.7771/1481-4374.2234]

Werghi, N., Xiao, Y.J., Siebert, J.P., 2006. A functional-based segmentation of human body scans in arbitrary postures. *IEEE Trans. Syst. Man Cybern. B*, **36**(1):153-165. [doi:10.1109/TSMCB.2005.854503]

Wuhrer, S., Ben Azouz, Z., Shu, C., 2010. Semi-automatic prediction of landmarks on human models in varying poses. Proc. Canadian Conf. on Computer and Robot Vision, p.136-142. [doi:10.1109/CRV.2010.25]

Zhang, H., Song, Y.H., Chen, Z., *et al.*, 2012. Chinese shadow puppetry with an interactive interface using the Kinect sensor. Proc. Computer Vision, p.352-361. [doi:10.1007/978-3-642-33863-2_35]

Zhu, Y.B., Li, C.J., Shen, I.F., *et al.*, 2003. A new form of traditional art: visual simulation of Chinese shadow play. Proc. ACM SIGGRAPH Sketches & Applications, p.1. [doi:10.1145/965400.965458]